Residential Home Decarbonization Using Advanced Micro-CHP

Zhiming Gao, PhD
ASHRAE Member

Philip Zoldak, PhD
ASHRAE Member

Maysam Molana, PhD
ASHRAE Member

Jacques Beaudry-Losique
ASHRAE Member

ABSTRACT

An efficient micro-combined heat and power (CHP) prototype was developed to provide heat and electricity for single-family homes and light commercial buildings. The unit can be installed independently at the point of energy consumption. Consequently, it enables cost-effectively and flexibly matching heat and electrical loads, simplifying distribution and installation processes, and recovering and storing waste heat as hot water. The analyzed results show that the micro-CHP using natural gas as fuel achieves 10.68%–32.80% CO_2 reduction in the selected five home applications. The potential effect of H_2 on decarbonization of these home was also evaluated, finding that the micro-CHP using a blended fuel with H_2 and natural gas can further reduce CO_2 emissions. However, the 50% CO_2 reduction in the micro-CHP requires at least 70%–90% of H_2 in the blend with natural gas. Overall, the micro-CHP technology demonstrates a solid potential to accelerate micro-CHP adoption in residential and light commercial markets, thereby promoting broader micro-CHP acceptance and use in the future for building decarbonization.

INTRODUCTION

Buildings often use substantial amounts of heat and electricity simultaneously. Conventional power plants typically lost two-thirds of the energy as waste heat during electricity generation [Martinez et al., 2017]. Additional energy losses occur during the distribution of electricity to end users. Unlike conventional power plants, combined heat and power (CHP) is a decentralized energy-efficient technology that generates electricity closer to the site of energy consumption while also capturing heat that would otherwise be wasted. This unique CHP feature contributes to sustainable building solutions, especially with the application of micro-CHP systems that can decentralize heat and electricity production directly at a consumption location.

Most commercial micro-CHPs employ internal combustion engines (ICEs) [Taie et al., 2019; Glenergy, 2016]. However, current ICE technologies in micro-CHP applications do not achieve more than 30% electrical efficiencies [Barbieri and Spina, 2012]. Developing novel technologies that enhance the efficiency and cost effectiveness of micro-CHPs is important for extending their market penetration. In opposed-piston engines (OPEs), the cylinder head is replaced by a second piston so that the two pistons move toward each other during compression. This unique configuration improves the stroke-to-bore ratio, reduces the surface area-to-volume ratio, and reduces heat transfer losses [Zhao et al., 2021; Zoldak, 2023]. OPEs enable 60% fewer parts per engine unit, significantly lowering the cost of OPEs. A compact OPE enables efficient, low-cost micro-CHPs.

Dr. Zhiming Gao is a senior R&D staff at Oak Ridge National Laboratory. Dr. Philip Zoldak is Engineering VP and a Technology Leader at Enginuity Power Systems, Dr. Maysam Molana is a senior research fellow at Enginuity Power Systems, and Mr. Jacques Beaudry-Losique is CEO of Enginuity Power Systems

This paper introduces a novel micro-CHP prototype using a gaseous-fueled, opposed-piston four-stroke (OP4S) engine to simultaneously provide heat and electricity to single-family houses [Gao et al., 2023]. The micro-CHP prototype aims to enable low-cost flexible matching of thermal and electrical loads and to reduce the complexity of distribution and installation by recovering and storing waste heat as hot water. The novel design will promote micro-CHP acceptance in the US residential and light commercial markets, given its low cost and drop-in replacement feature. This paper describes the prototype of the micro-CHP system and its performance evaluation in efficiency and decarbonization.

METHODOLOGY AND EXPERIMENTAL SETUP

Micro-CHP development

The micro-CHP unit includes a 0.5 L (0.132 gal) OP4S, a generator with an efficiency of 90%, a 196.8 L (52 gal) water tank, and external accessory components consisting of a rectifier, an inverter, a 15.2 kWh battery energy system, and hot water supply and space-heating application systems [Gao et al., 2024]. Figure 1 shows the micro-CHP unit, which can operate with natural gas and hydrogen to generate AC electricity and hot water at the same time. The waste heat in the hot coolant and exhaust flow is recovered to generate hot water stored in the water tank. The hot water serves as both a hot water supply and a space-heating application in a building.

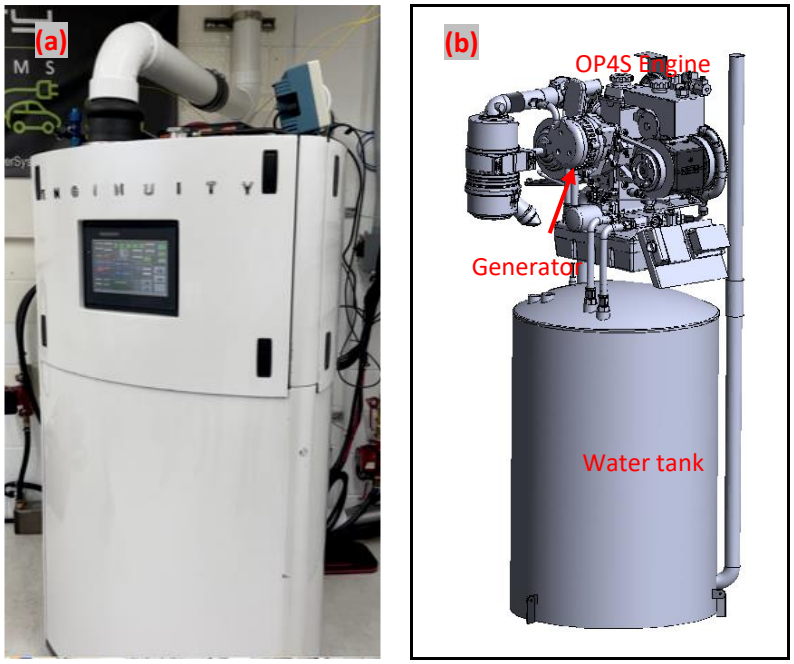

Figure 1 The integrated micro-CHP system: (a) the external view and (b) the internal carton view of the system architecture.

The OP4S operates with premixed natural gas or gaseous fuels containing hydrogen. Figure 2 shows the external configuration. In the OP4S, two pistons share one cylinder. The opposed pistons move toward one another and meet at the top center. As the pistons approach each other at the top of each stroke, the premixed gas fuel is ignited by a spark plug in the cylinder. The combustion converts fuel potential energy to work and pushes the pistons apart. The mechanical power is transported to the generator and produces AC electricity. Unlike conventional ICEs, the OPE has no traditional cams and no cylinder head; therefore, it is simpler and cheaper to manufacture, assemble, and operate, and it enables higher efficiency owing to less heat loss and less friction [Gao et al., 2015; Zoldak et al., 2023].

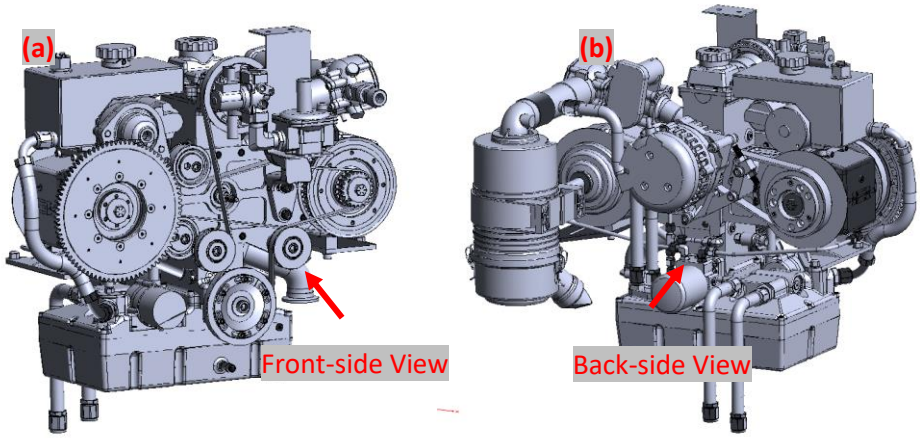

Figure 2 Configuration of the OP4S used in the micro-CHP: (a) front-side view and (b) back-side view.

The micro-CHP captures waste heat effectively and produces hot water through a coolant flow coil and an exhaust gas coil embedded within the water tank. Hot water is stored in the water tank and can be used for domestic hot water supply and space heating. Figure 3 illustrates the waste heat recovery configuration, which has a large-diameter helical coil for hot exhaust heat recovery and a smaller-diameter inner coil for hot coolant heat recovery.

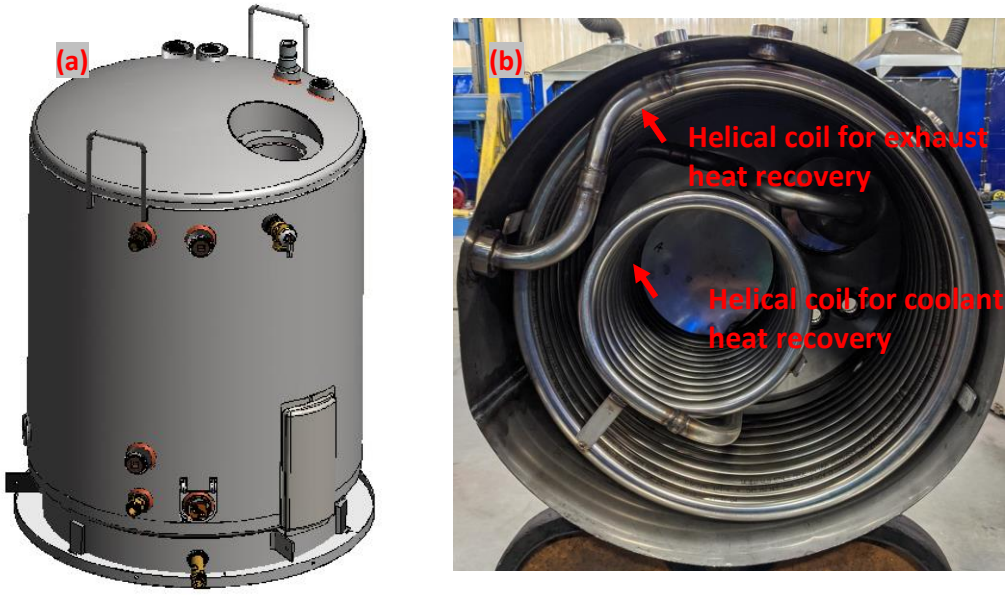

Figure 3 Micro-CHP waste heat recovery component: (a) external configuration and (b) internal architecture showing the helical coils for exhaust and coolant waste heat recovery.

Micro-CHP Experimental Setup

The micro-CHP prototype was tested in EPS's testing facility. In the testing system, a simulated hot water supply load is applied using a compact plate heat exchanger, which transfers heat from the micro-CHP's water tank to the testing facility's cooling loop. The cooled return water is then sent back to the water tank. For the space-heating application, hot water is directly supplied from the micro-CHP's water tank to a space-heating device. To facilitate comprehensive data collection for the analysis, thermocouples and flow meters (for air, fuel, and coolant flows) and sensors for

measuring electrical current and voltage were installed throughout the system. Main measurements include fuel consumption, battery current and voltage, lambda or O_2 sensor data, exhaust temperatures at the water tank inlet and outlet, coolant temperatures and flows at the water tank inlet and outlet, household hot water flow and temperature, and space-heating water flow and temperature. All sensor data are captured by the PLC modules, which, together with the ECU, control the micro-CHP system.

Efficiency Analysis Methodology

Based on the first law of thermodynamics, the electric efficiency, η_e, is defined as the AC electrical energy rate, $\dot{W}_e$, divided by the fuel energy consumption rate, $\dot{Q}_{f,LHV}$, based on the fuel low heating value (LHV). The AC electric efficiency, η_e, can also be descried as a function of engine efficiency and generator efficiency, given by Eq. (1). The overall CHP efficiency, η_{chp}, is evaluated by considering the recovered thermal energy flow, $\sum \dot{Q}_{th}$, and electrical energy rate, $\dot{W}_e$, and then dividing that by the fuel energy consumption flow, $\dot{Q}_{f,HHV}$, based on the fuel higher heating value (HHV). The calculation is given Eq. (2).

$$\eta_e = \frac{\dot{W}_e}{\dot{Q}_{f,LHV}} = \eta_{eng} \cdot \eta_{gen} \quad (1)$$

$$\eta_{chp} = \frac{\dot{W}_e + \sum \dot{Q}_{th}}{\dot{Q}_{f,HHV}} \quad (2)$$

Decarbonization Analysis Methodology

The decarbonization benefits of the micro-CHP prototype performance in building applications were simulated based on five single-family homes, which were selected, respectively, from cities in five states in the United States. In the simulations, the micro-CHP is assumed to replace a residential furnace, water heater, and grid power supply. The electricity and natural gas consumption for space and water heating in these homes is based on real-world data available from the EnergyPlus residential energy consumption database [EnergyPlus, 2024]. Also, in the simulations, the micro-CHP operates optimally by switching between stoichiometric and lean modes to maximize CO_2 emissions reduction while meeting heat and electricity demands in each home. In each micro-CHP operation mode, the electricity output is considered to satisfy household power demand. However, if the micro-CHP electricity output falls short of meeting household power demand, grid electricity buffers the excess power demand. Similarly, the micro-CHP waste heat is assumed to meet household thermal energy demand for space and water heating typically fulfilled by natural gas. If the micro-CHP waste heat can't satisfy thermal energy demand, the micro-CHP uses its electricity output, along with grid electricity, to buffer the additional thermal energy demand. Carbon emissions from the micro-CHP are simulated based on direct carbon emissions associated with natural gas consumption and indirect carbon emissions imported from the grid. As a benchmark, carbon emissions from a conventional house that uses electrical components and natural gas devices (e.g., gas furnace and water heater) were also calculated to evaluate the micro-CHP's potential benefits.

RESULTS

Micro-CHP Efficiency

The micro-CHP is capable of operating at the stoichiometric or lean combustion mode. In the lean mode, the control module in the OP4S engine used the lambda sensor and intake port actuator to maintain a 30% excess of air, and the ignition timing for all lean modes was advanced by approximately 10°CA to maximize engine brake thermal efficiency

compared with the stoichiometric modes. Table 1 shows the key performing parameters of the micro-CHP under stoichiometric and lean modes. The studies use natural gas. Both the cases run around 2,850–2,877 rpm. The lean mode achieves 35.21% AC electrical efficiency, compared with a lower efficiency of 17.17% for the stoichiometric mode. However, the total CHP energy efficiency of the lean mode is 86.4%, which is less than 93.2% efficiency for the stoichiometric mode. Figure 4 shows the details of energy flow of the micro-CHP system running at the stoichiometric and lean modes.

Table 1. Thermal Energy Performance of the Micro-CHP Under the Stoichiometric and Lean Modes*

Combustion Mode	Stoichiometric Mode	Lean Mode
Engine speed (rpm)	2877	2850
Fuel input (HHV) (kW)	25.76	18.68
Fuel input (LHV) (kW)	23.27	16.87
AC power (kW)	3.89	5.93
AC efficiency (%)	17.17	35.21
Total CHP energy efficiency (%)	93.23	86.40
Engine-out exhaust (kW)	19.07	7.08
Exhaust waste recovery (kW)	8.40	5.52
Coolant waste recovery (kW)	11.72	4.68
Exhaust temperature at exit of water tank (°C)	31.3	47.7

*Fuel: natural gas

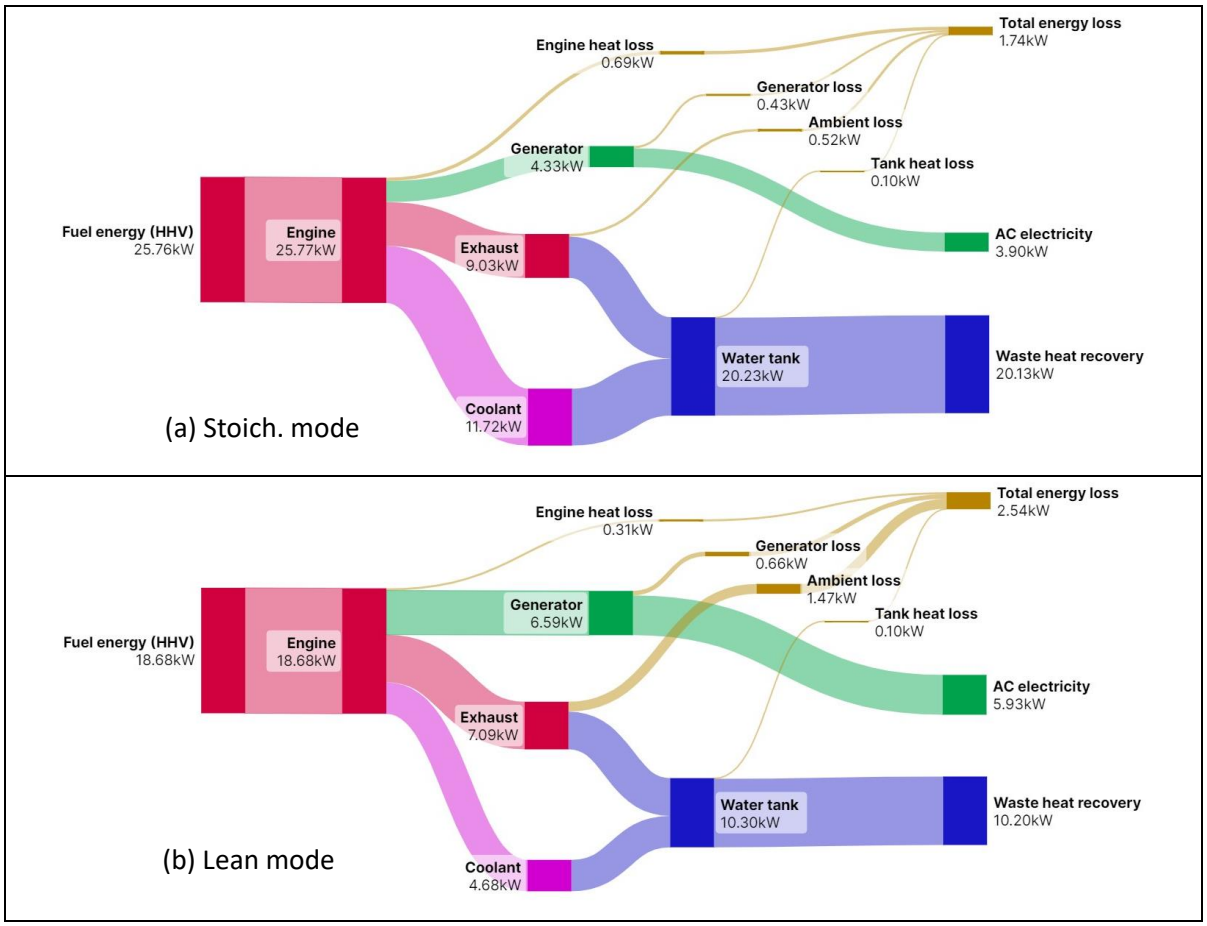

Figure 4 Energy flow of the micro-CHP system in the (a) stoichiometric and (b) lean modes.

Two factors result in lower total micro-CHP efficiencies in lean combustion modes. First, lean combustion modes lead to exhaust temperatures at the water tank exit at 47.7°C (117.9°F), indicating potential for improvement in the thermal energy control system for enhanced waste heat recovery. Second, lean combustion modes inherently lead to a lower ratio of moisture to dry air, increasing uncondensed water in the exhaust flow rejected to ambient conditions and causing higher latent heat loss. In these studies, the latent heat loss owing to uncondensed water vapor in the lean modes is ~6.4% of HHV fuel energy. The loss in the stoichiometric modes is 2.2% of HHV fuel energy with the exhaust temperature at the exit of the water tank below 40°C (104.0°F). Details are shown in Figure 5.

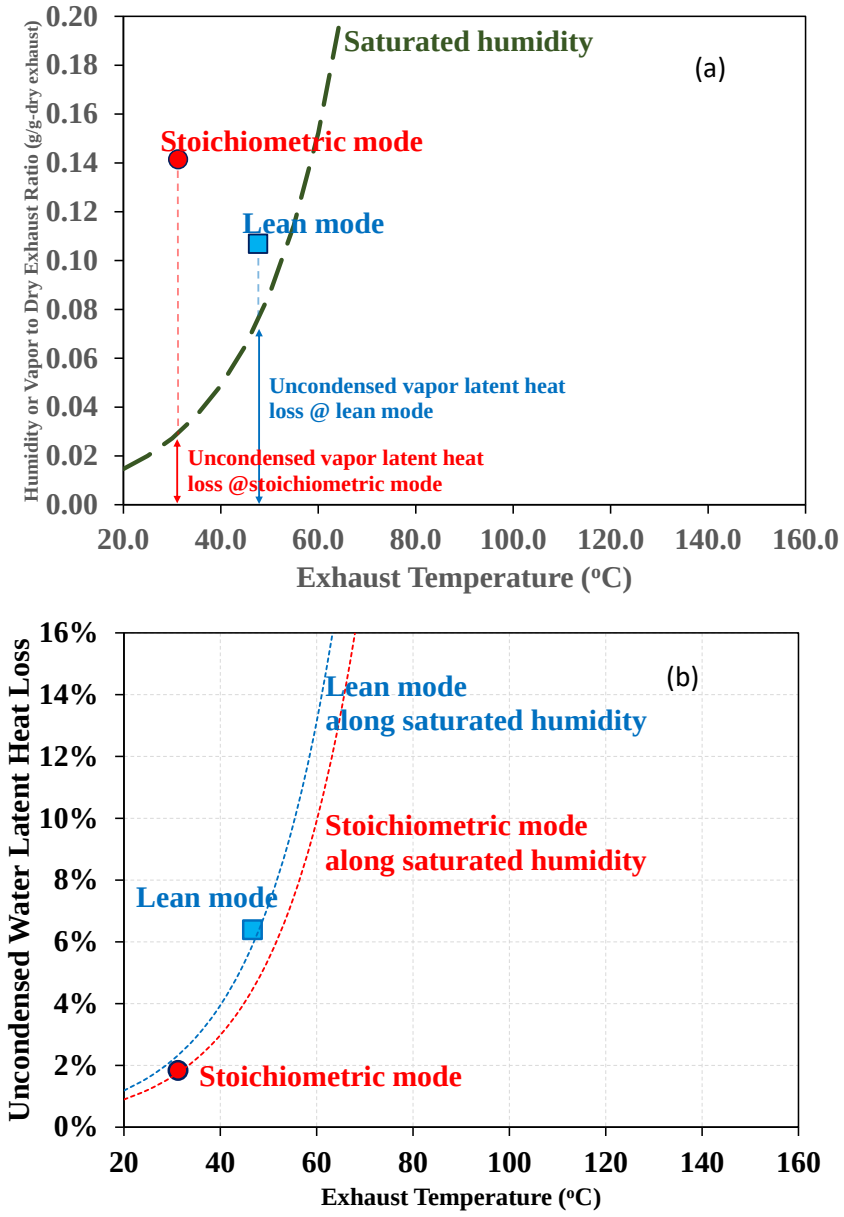

Figure 5 Comparison of (a) vapor to dry exhaust ratio and (b) latent heat loss owing to uncondensed water vapor between lean and stoichiometric modes. In Figure 5(b), the percentage of the uncondensed water latent heat loss is based on HHV fuel energy. Note: red circle is the stoichiometric mode, and blue square is the lean mode.

The micro-CHP system's performance was compared with that of commercial or prototype micro-CHPs with

electrical power of less than 10 kW (34.12 kBTU/hr). The results are shown in Figure 6. All the cases use natural gas. The observation reveals that up to 35.2% of AC electrical efficiency demonstrated by the developed micro-CHP operating at lean mode exceeds the upper boundary of 30% for an ICE-based micro-CHP, as reported in the public domain. The overall micro-CHP efficiency of up to 93.2% at stoichiometric mode is still comparable to the maximum micro-CHP efficiencies reported in the public domain, although the lean combustion mode achieves less than 90% of the overall micro-CHP efficiency. In addition, the max power enabled in the current micro-CHP is also marked as the spot of max power, which runs at stoichiometric mode, in Figure 6. The max power operation does not achieve highest electrical or total CHP energy efficiencies.

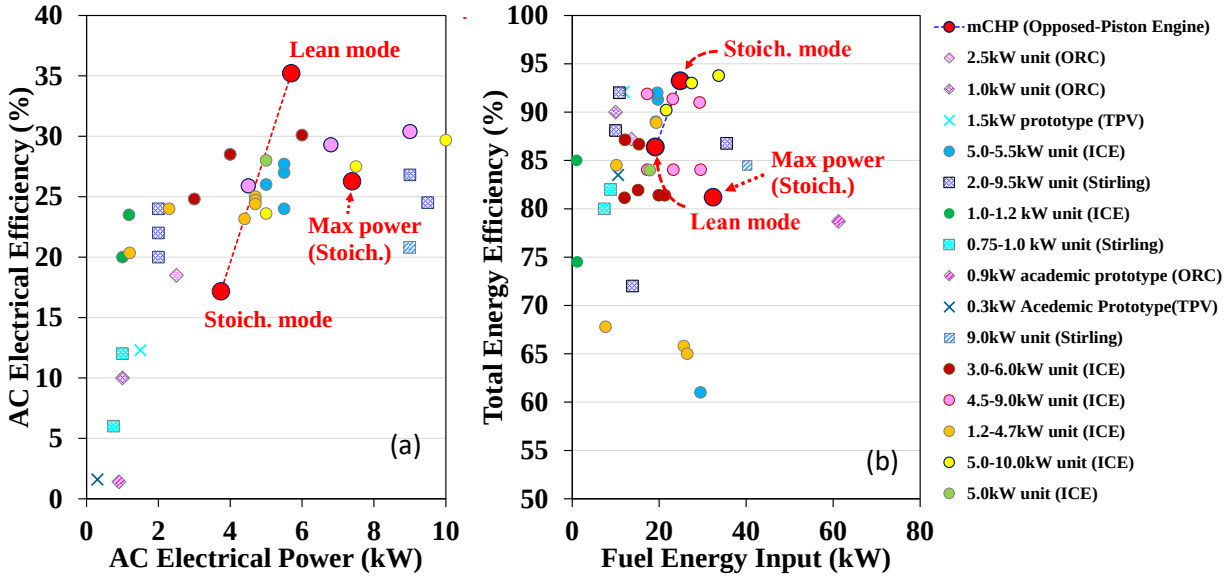

Figure 6 Efficiency comparison between the current micro-CHP and micro-CHPs available in the public domain. (a) electrical efficiency and (b) Total CHP energy efficiency.

Discussion: Building Decarbonization Using the Micro-CHP

Five single homes from Anchorage (Alaska), Detroit (Michigan), Boulder (Colorado), Kansas City (Missouri), and Lexington (Kentucky) were selected to simulate the decarbonization benefits of the micro-CHP in residential applications. The results are shown in Table 2. The conventional homes were assumed to adopt gas furnaces for space heating and gas water heaters for water heating while use grid power. The new homes adopt micro-CHPs to meet house power and thermal energy demand and use grid power to buffer additional energy need if necessary. In the study, the fuel used in the micro-CHP is natural gas, and the carbon intensity of electricity for each conventional home is based on EIA's data [EIA, 2024]. The detailed decarbonization varies with these locations' carbon intensity of electricity generation and local climate conditions enabling the optimal utilization of electricity and waste heat from the micro-CHP. The micro-CHP using natural gas as fuel achieves 10.68%–32.80% CO_2 reduction (i.e., 1.29–4.94 ton or 2,838–10,868 lb per year). The results indicate that significant CO_2 reduction occurs in Colorado, Missouri and Kentucky because most power plants in these locations currently are coal-fired, leading to higher carbon intensity of electricity generation. Thus, this new micro-CHP technology is expected to accelerate micro-CHP adoption in residential and light commercial markets, promoting broader micro-CHP acceptance and use in building decarbonization in the future.

Table 2 further shows potential effects of H_2 on building decarbonization. In the studies, a blended-gas fuel consisting of 25 mol % natural gas and 75 mol % H_2 is considered, and the micro-CHP using the blended natural gas and H_2 is assumed to achieve the same electrical efficiency and overall micro-CHP efficiency as that of natural gas. The results

reveal that the micro-CHP can achieve 33.98%–51.42% CO_2 reduction. Compared with natural gas, the density of H_2 is around 11% of the former—i.e., 0.090 kg/m³ (5.61e-3 lb/ft³) of H_2 vs. 0.800 kg/m³ (4.99e-2 lb/ft³) of natural gas. That leads to the carbon mass-basis percent remaining at 55.95% even in the blend of 25 mol % natural gas and 75 mol % H_2, compared with 75.70% carbon mass-basis of natural gas. Figure 7(a) shows the carbon percentage drop significantly if H_2 in the blended gas with natural gas is above 90%. Therefore, Figure 7(b) shows that a 50% CO_2 reduction in the micro-CHP requires at least 70%–90% of H_2 in the blended gas with natural gas.

Table 2. The Decarbonization of Micro-CHP Applications in the Selected Households

Mode	1 year conventional home			1 year new home using micro-CHP			CO2 reduction	
Location	Electricity (MWh)	NG (MWh)	CO2e (ton)	Gas Energy (MWh)	CO2e (ton) using NGs	CO2e (ton) using 25% NG/ 75% H2*	CO2e savings % (NG)	CO2e savings % (25% NG/ 75% H2*)
Anchorage, AK	9.32	55.02	15.63	71.82	13.50	9.98	13.58%	36.16%
Detroit, MI	9.03	40.09	12.07	57.34	10.78	7.97	10.68%	33.98%
Boulder, CO	9.01	34.55	11.69	51.96	9.77	7.22	16.44%	38.22%
Kansas City, MO	12.89	20.66	14.40	53.17	9.99	7.38	30.58%	48.72%
Lexington, KY	12.31	19.66	14.41	50.38	9.47	6.99	32.80%	51.42%

* Mole basis; NG: Natural gas; carbon intensity of electricity for each conventional home is based on EIA's data [EIA, 2024]

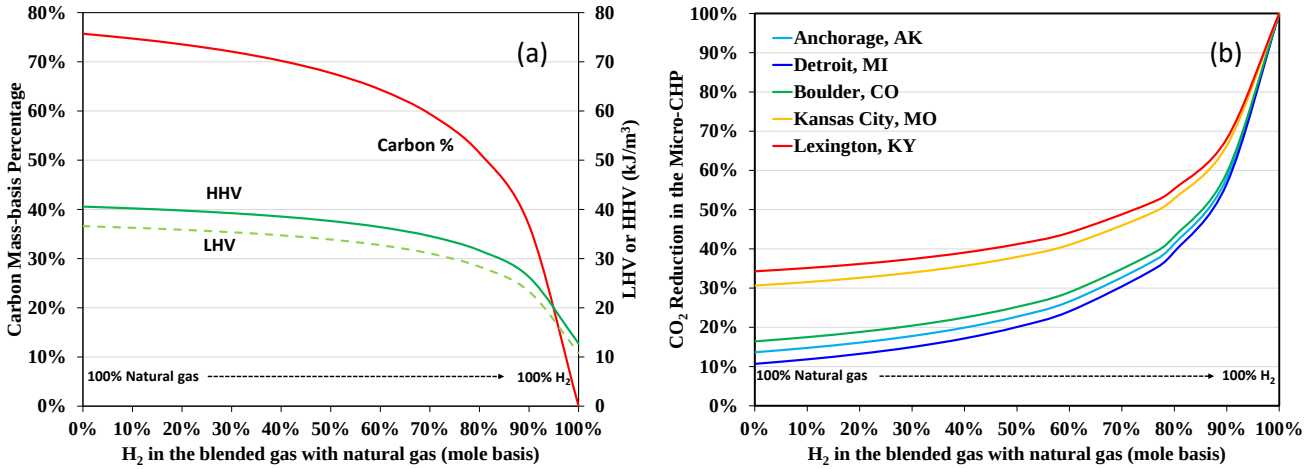

Figure 7 (a) The carbon mass-basis percentage and heating values of the blended hydrogen and natural gas, and (b) the effect of H_2 in the blended gas on CO_2 reduction in the micro-CHP.

CONCLUSION

An efficient micro-CHP was developed to achieve up to 35.2% of fuel-to-electricity efficiency at the lean combustion mode, exceeding the conventional micro-CHP's fuel-to-electricity efficiency limit of 30%. At the stoichiometric mode, the unit achieves much less electrical efficiency, but the overall micro-CHP efficiency of up to 93.2% is comparable to that of the maximum micro-CHP efficiencies reported in the public domain. Moreover, the OP4S engine used in the micro-CHP enables 60% fewer parts per engine unit, thus lowering materials and manufacturing costs.

Five single homes were selected to simulate the decarbonization benefits of the micro-CHP in residential applications. The micro-CHP using natural gas as fuel achieves 10.68%–32.80% CO_2 reduction. The potential effect of H_2 on decarbonization of these building was also explored. The micro-CHP using a blended fuel with H_2 and natural is expected to further reduce CO_2 emissions, but 50% CO_2 reduction in the micro-CHP requires at least 70%–90% of H_2 in the blend with natural gas because of the lower density of H_2 compared with natural gas.

Overall, the micro-CHP advances the state-of-the-art of the technology and will play a critical role for the energy needs of remote and underserved communities, especially during unexpected severe weather when both electricity and heat are most needed.

ACKNOWLEDGMENTS

The author would like to acknowledge the US Department of Energy, Office of Energy Efficiency & Renewable Energy, the Building Technologies Office, and the ORNL Climate Change Science Institute (CCSI) initiative called Science and Technology for Applied Regional Solutions (CCSI STARS). Also, the author thanks ORNL and EPS colleagues for help in the work and Wendy Hames of ORNL for technical editing.

NOMENCLATURE

η_e	=	Electric efficiency
η_{chp}	=	Overall CHP efficiency
$\dot{w}_e$	=	AC electrical energy rate
$\dot{Q}_{f,LHV}$	=	Low heating value
$\dot{Q}_{f,HHV}$	=	High heating value
$\sum \dot{Q}_{th}$	=	Recovered thermal energy flow

REFERENCES

Barbieri, E. S., Spina, P. R. 2012. Venturini M. Analysis of innovative micro-CHP systems to meet household energy demands. Appl Energ 97: 723–733.

EnergyPlus. 2024. https://energyplus.net/. [accessed August 28, 2024].

EIA. 2024. https://www.eia.gov/environment/emissions/state/. [accessed August 28, 2024].

Gao, Z., et al. 2015. Drive cycle simulation of high efficiency combustions on fuel economy and exhaust properties in light-duty vehicles. Appl. Energy 157:762–776.

Gao, Z., Zoldak, P., Beaudry-Losique, J., Mannarino, T., et al. 2023. Development and testing of residential micro-CHP powered by opposed piston engine. ORNL/TM-2023/2883. Oak Ridge, Tennessee: Oak Ridge National Laboratory.

Gao, Z., Zoldak, P., Beaudry-Losique, J., Mannarino, T., et al. 2024. Development of a micro-combined heat and power powered by an opposed-piston engine in building applications. Nature Communications 15(1):4404.

Glenergy. 2016. Dachs—Mini CHP Combined Heat and Power Technical Specification, http://glenergy.ie/wp-content/uploads/2016/10/Dachs_-_Mini_CHP_Technical_specification.pdf. [accessed August 28, 2024].

Martinez, S., Michaux, G., Salagnac, P., Bouvier, J. L. 2017. Micro-combined heat and power systems (micro-CHP) based on renewable energy sources. Energ Convers Manage 154: 262–285.

Taie, Z., Hagen, C. 2019. Experimental thermodynamic first and second law analysis of a variable output 1–4.5 kWe, ICE-driven, natural-gas fueled micro-CHP generator. Energ Conv Manage 180: 292–301.

Zhao, W., Li, R., Li, H., Zhang, Y., et.al. 2021. Numerical analysis of fluid dynamics and thermodynamics in a Stirling engine. Appl Therm Eng 189: 116727.

Zoldak, P., Douvry-Rabjeau, J. Zyada, A. 2023. Potential of a hydrogen-fueled opposed piston four stroke (OP4S) engine. SAE Technical Paper 2023-01-0408.